scientific reports



OPEN

Enhanced photocatalytic degradation of 2,4-dichlorophenoxyacetic acid from freshwater and industrial wastewater using TiO₂-CuO-clay soil nanocomposites

Sisay Demissie Geda^{1,3}, Tadesse Alemu Terfie^{01™} & Mekonnen Abebayehu Desta²

2,4-Dichlorophenoxyacetic acid (2,4-D) is a synthetic herbicide used to control weeds and enhance agricultural productivity. However, it is toxic and carcinogenic, posing significant risks to environmental pollution and human health. This study investigates the effectiveness of TiO₃-CuO-clay soil nanocomposites in the photocatalytic degradation of pesticides from Ziway Lake and industrial wastewater. The two sets of composites were synthesized with different concentrations of TiO₂-CuOclay soil: the first with a ratio of 2:3:7 (TiO₂, CuO and clay soil), and the second with a ratio of 4:3:5 (TiO₂, CuO and clay soil). The mixture was treated with microwave digestion at 150 °C for 10 min, followed by filtration and calcination at 720 °C for 6 h in a muffle furnace. The morphology and the particle size of the nanocomposites were characterized using XRD, SEM, FTIR and BET techniques. The pesticide degradation from Ziway Lake and pesticide factory effluents was carried out using a UV-vis spectroscopy lamp with a wavelength of 280 nm, with samples retained for 2, 5, 7, and 9 h. The removal efficiency of 2,4 D was then analyzed by HPLC. The results revealed that the degradation efficiency of TiO₃-CuO-clay soil composite was 96.18% and 99.84% for surface water and pesticide factory effluent, respectively. The removal efficiency increased with longer contact duration, higher light intensity, and greater composite concentrations. The study demonstrates that TiO₂-CuO-clay soil composites were an effective technology for pesticide degradation in surface water and industrial wastewater.

Keywords 2,4-D based pesticides, Degradation, Pesticides effluent, Photocatalysis, TiO₂-CuO-clay soil composite

Abbreviations

BET Brunauer-Emmett-Teller
CRV Central RIFT VALLEY

DDE Dichlorodiphenyldichloroethylene

EF Environmental functions

HPLC High-pressure liquid chromatograph

L-H Langmuir-Hinshelwood PEG Poly (ethylene glycol)

SAED Selected area electron diffraction SEM Scanning electron microscope

¹Center for Environmental Science, College of Natural and Computational Sciences, Addis Ababa University, P. O. Box 1176, Addis Ababa, Ethiopia. ²Department of Chemistry, College of Natural and Computational Sciences, Addis Ababa University, P. O. Box 1176, Addis Ababa, Ethiopia. ³Chemical and Construction Inputs Industry Research Development Center, Manufacturing Industry Development Institute, P. O. Box 4124, Addis Ababa, Ethiopia. □Cemail: tadesse.alemu@aau.edu.et

SSIF Small-scale irrigated farms
UV-VIS Ultra violet-visible spectroscopy

XRD X-ray diffraction

2,4-D 2,4-Dichlorophenoxyacetic acid

Ha Hectares

Herbicides are a sub-group of pesticides and played a significant role in ensuring food security over the past 5 decades by boosting agricultural output and controlling weeds^{1,2}. The increased agricultural productivity has significantly benefited the economies of both rural and urban areas throughout the world. The Foresight Commission studies have highlighted 40 initiatives and programs across 20 nations where sustainable intensification began to take shape in the 1990s and 2000s^{3,4}. However, the intensification of agricultural practices to meet the rising global food demand has resulted in an increased contamination of soil, water and aquatic ecosystems⁵. Many of these chemicals are ultimately lost to the environment through processes such as volatilization, hydrolysis, photolysis, or microbial activity⁶. The runoff of pesticides contaminate other bodies such as lakes and rivers, disrupting their ecological functions and posing health risks^{7,8}.

The ongoing agricultural transformation in Africa, particularly in Sub-Saharan Africa, has resulted in an increase in anthropogenic pollution due to pesticide misuse, and rising serious environmental health concerns^{9,10}. Ethiopia used a total of 5.2×10^3 tons of 2,4-D between 2000 and 2016^{11} . Ziway Lake is an essential freshwater resource in the country and is used for multiple purposes, including irrigation, fishing, water supply, and recreation¹². Since 1973, the area dedicated to irrigated agriculture in the catchment has expanded to 5000 hectares. By 2006, land use data indicates that small-scale agriculture covered approximately 7300 hectares, which has been contaminated by organochlorine pesticides in the Meki River catchment. These pesticides include dieldrin, heptachlor, chlordane, endosulfan II, delta-benzene hexachloride (dBHC), Atrazine, Aldrin, 2,4-D, dimethoate, and endosulfan-s⁷. The extent of pollution indicates significant land degradation and environmental dysfunction.

Most of the studies in Ethiopia focus on the detection of pesticides in soil and water bodies. Studies conducted in the past have demonstrated that, Ziway Lake is highly contaminated due to agricultural runoff into the lake 13 . The extensive use of agrochemical inputs in the irrigation and horticultural industry has been linked with negative environmental and health impacts 7 . The pesticide monitoring study 14 found that out of 30 different pesticides, one was detected in concentrations exceeding $0.1 \,\mu\text{g/L}$ in Ziway Lake. The local population relies on Ziway Lake for drinking water and filters water using sheets (a single garment) to remove particulate matter. The current conventional agrochemical industrial wastewater treatments, such as primary and secondary treatments, in the country, are inadequate in removing pesticide residue to the acceptable standard, putting the community and the environment at risk.

2,4-Dichlorophenoxyacitic acid (2,4-D) is one of the most widely used herbicides since its introduction in the 1940s¹⁵. Its extensive use and toxicological effect shows its significance in controlling broadleaf weeds and crop resistance. However, recent toxicological studies have raised about the adverse effects of 2,4-D on water bodies, air quality, non-target organisms, and human health¹⁶. In Ethiopia, a huge amount of 2,4-D is produced in the Adami Tulu Pesticide Processing factory and is a widely used systemic herbicide designed to control broadleaf weeds. This suggests that the urgent need for detection and treatment methods to monitor and mitigate the environmental and health risks associated with this herbicide.

Research conducted on herbicide treatment in developing countries, including Ethiopia, remains limited. Nonetheless, implementing pesticide treatment methods is essential for treating contamination in water bodies resulting from agricultural practices and industrial activities. Among these methods, photocatalytic degradation has gained significant attention due to its effectiveness in removing both organic and inorganic contaminants, including harmful pesticides such as 2,4-D and atrazine^{17,18}. The process utilizes metals and their compounds, such as titanium dioxide (${\rm TiO_2}$), graphite carbon nitride (${\rm g-C_3N_4}$) and Ag@Mg₄TaO₉, as a photocatalyst, which activated by light, that generates highly reactive hydroxyl radicals capable of breaking down organic contaminants into harmless by-products¹⁹. However, the treatment methods of pesticide-contaminated wastewater at the source and water for domestic use from Ziway Lake were not studied. Therefore, the objective of this study was to investigate the photocatalytic degradation of 2,4-D-based pesticides using a ${\rm TiO_2-CuO-clay}$ soil nanocomposite. The combination of ${\rm TiO_2}$, ${\rm CuO}$, and clay is expected to outperform ${\rm TiO_2}$ or ${\rm CuO}$ used alone, due to the synergistic effects, increased surface area, and better light absorption. The combination of ${\rm TiO_2}$, ${\rm CuO}$, and clay is expected to outperform ${\rm TiO_2}$ or ${\rm CuO}$ used alone due to the synergistic effects, increased surface area, and better light absorption.

Materials and methods Chemicals and instruments

Laboratory-graded commercial chemicals including titanium dioxide (TiO_2 98%), hydrogen peroxide (H_2O_2 98%), sodium hydroxide pellets (NaOH 98%, Himedia Laboratory Pt, India), hydrochloric acid (HCl, RFCL limited, new Delhi, India), Sulfuric acid (H_2SO_4 98.0% Lobal chemical, India), Acetonitrile, methanol (all HPLC grade), and Dichlorophenoxyacetic acid (2,4-D, 99%, Tianjin chemical reagent, China) were used for this investigation²⁰. Additionally, copper oxide (CuO), copper(II) acetate, clay soil and 2,4-D pesticides were used without further treatment.

Polyethylene bottles, drying Oven (model GX65B), SHO-2D Wise shaker, SX-2.5-10 muffle furnace, EFA-6UDRVW-8 hood, JENWAY 3510 pH meter), high-pressure liquid chromatography (HPLC), scanning electron microscopy (SEM), X-ray diffraction (XRD), UV reactor, Fourier Transform Infrared (FT-IR) and Brunauer–Emmett–Teller (BET) were used. The study employed SEM to analyze the particle morphology of the catalysts.

The SEM utilized was a field emission high-vacuum system, specifically the SED PC-std model, operating at 15 kV with a magnification of $200 \times (44 \text{ mm})$.

Description of the study area

The study was conducted at Ziway Lake, and Adami Tulu pesticide factory is located 168 km south of Addis Ababa, the capital city of Ethiopia. Ziway Lake is found in the central Rift Valley (CRV) East Shewa Zone Oromia, and covering an area of 7148 km², it is located between the latitude of 7° 22′ 36″ N and 8° 18′ 21″ N and 37° 53′ 40″ E and 39° 28′ 9″ E longitude. The lake is primarily fed by tributaries including the Meki River, Bulbula River, and Ketar River. However, the lake faces significant environmental challenges due to pollution from various non-point sources including pesticide runoff, nutrient loading, agricultural pesticides, industrial activities, and urbanization.

Sample collection

Five liters of water samples were collected from Ziway Lake and the Adami Tulu pesticide factory by using the grab sampling technique in polyethylene plastic containers to analyze pesticide concentrations. The samples were collected in February 2023. Sampling locations were systematically selected based on spatial variations in the water stream and irrigation system to ensure representative sampling. Additionally, clay soil for composite preparation was collected from the Addis Ababa-Asko area.

Purification of clay soil

The collected clay soil was dried for 30 min (Dry oven GX-65B), ground (Nima Japan NM-8300), and passed through a 0.5 mm sieve (ISO 3310-1)^{21,22}. The ground clay soil was dispersed in hydrogen peroxide solution for 20 min at 30 °C to remove organic carbon. Oxidation of soil organic matter occurred during H_2O_2 reactions with clay soil, and the pH content had a significant impact on the breakdown of organic matter. Subsequently, the suspensions were evaporated and allowed to cool. The slurry was then rinsed with acidified distilled water (pH \approx 4) to protect it from any contaminants while being continuously shaken at 300 rpm (Wise shaker, SHO-2D) for 30 min to eliminate any remaining inorganic carbon. Finally, it was allowed to settle for 3 h. After carefully removing the floating materials and supernatant from the settled clay, the remained was transferred to a 500 mL beaker and dried at 105 °C overnight. Finally it was ground for 5 h in a ball mill.

Synthesize of TiO₂–CuO–clay soil composite

The TiO₂–CuO–clay soil nanocomposite was developed following the process of clay soil preparation. Two procedures were used to synthesize the oxide of TiO₂–CuO–clay soil composite photocatalyst systems. First, a 5% aqueous solution of Copper(II) acetate was prepared. Two different concentrations of the composites were formed using different amounts of TiO₂, CuO, and clay soil. The first composite consisted of 2 gof TiO₂, 3 gof CuO, and 7 gof nano clay soil, while the second composite contained 4 gof TiO₂, 3 gof CuO, and 5 gof clay soil (Table 1). Each composite was dissolved in 25 mL of the 5% aqueous Copper(II) acetate solution. Additionally, 2 gof polyethylene glycol (PEG) was added to each mixture to enhance the bonding between the components of the composite. The ratio of TiO₂:CuO:clay soil composites of different concentrations were 2:3:7 and 4:3:5. These ratios were determined based on the adsorption capacity of the composite nanoparticles and existing studies. The mixture was stirred using a magnetic stirrer, and 1 M of sodium hydroxide solution was added to adjust the pH of the TiO₂–CuO–clay soil oxide to 12. Lastly, the mixture was treated with microwave treatment for 10 min at 105 °C with power of 300 W (SP-D80, CEM). The synthesized oxide system was washed three times with deionized water, filtered, and dried for 7 h at 70 °C based on Kubiak's²³ report and calcined in a muffle furnace for 6 h at 720 °C (muffle furnace model SX-2.5-10)²¹.

The UV-vis measurements were conducted using a Shimadzu UV-vis spectrophotometer, and the band gap energy was calculated using the Kubelka–Munk equation from reflectance spectra²⁴. Based on the experimental results of 2,4-D degradations, the ${\rm TiO}_2$ –CuO-clay soil composite had the best photocatalytic performance for UV-vis photocatalytic degradation of 2,4-D. Then, ${\rm TiO}_2$, CuO, and clay soil were synthesized with a molar ratio of 4:3:5 and calcined for 6 h at the temperature of 720 °C. Furthermore, the ${\rm TiO}_2$ –CuO-clay soil composite's photocatalyst performance, shape, crystalline nature, light absorbance behavior, and band gap energy were demonstrated via UV-vis, FT-IR, SEM, and X-ray diffraction (XRD).

The band gap energy of the ${\rm TiO_2-CuO-clay}$ soil composite was calculated using Kubelka–Munk band gap energy formula:

Composites	Catalysts and adsorbent	Quantity (g)	Percentage (%)
	TiO ₂	2	16.7
1st Composite	CuO	3	25
	Clay soil	7	58.33
	TiO ₂	4	33.33
2nd Composite	CuO	3	25
	Clay soil	5	41.7

Table 1. Composition ratios of TiO₂-CuO-clay soil composites.

$$K = \frac{(1-R)^2}{2R}$$

where K is the absorption coefficient and R is the reflectance of the material.

To calculate the band gap energy (E₂), the relationship can be drived from the Kubelka-Munk function: $E_g=\frac{1240}{\lambda}$ eV, where: E_g is the energy band gap of the material and λ is wave length of light. The percentage degradations of 2,4-D was calculated by:

$$R\left(\%\right) = \frac{Co - Cf}{Co} * 100$$

where R is concentrations of pesticides, Co is Initial concentration of pesticide, Cf is final concentration of pesticide.

The photocatalytic activity of TiO2-CuO-clay soil composite was compared with different ratios of photocatalysis under UV-vis spectroscopy light.

Photocatalytic degradation of 2,4-D experiment

The composite of TiO₂-CuO-clay soil, weighing 2 g, was prepared and mixed with 1 L of contaminated water for ultraviolet (UV) treatment. The UV lamp was then applied to the mixture to facilitate the breakdown of pesticide molecules. After treatment, the sample was filtered to remove the solid composite, and the remaining solution was analyzed using high-performance liquid chromatography (HPLC) to determine the concentrations of 2,4-D following the photocatalytic process (Fig. 1). For the analysis of 2,4-D concentration, water and acetonitrile were used at a wavelength of 265 nm, and a flow rate of 0.8 mL/min. For the analysis of 2,4-D concentration, water and acetonitrile were used at a wavelength of 265 nm, and a flow rate of 0.8 mL/min.

Result and discussion

Synthesis and characterization of TiO₂-CuO-clay soil nanocomposite

The result showed that the UV-Vis photocatalysis of the TiO₃-CuO-clay soil composite required calcining the material for 6 h at 720 °C. The calcination process significantly alters the catalyst's crystalline structure, particle size, and surface morphology. Generally, the higher calcination temperatures can enhance crystallinity and improve photocatalytic activity. However, studies showed that excessively high temperatures may lead to particle agglomeration, which can reduce the effectiveness of photocatalytic degradation^{25,26}.

The calcination temperature plays a crucial role in determining the properties of the photocatalyst. At optimal temperatures, the material achieves a desirable balance between crystallinity and surface area, enhancing its ability to effectively degrade pollutants. According to the study by²⁷ showed that the transformation of the crystalline structure can facilitate better electron transfer and increase the formation of reactive species under UV illumination.

The size and shape of the catalyst particles are important for their photocatalytic performance. Smaller particles generally provide a larger surface area for reactions, while specific morphologies can influence light absorption and catalytic efficiency. However, a study reported that excessive heat can cause particles to clump

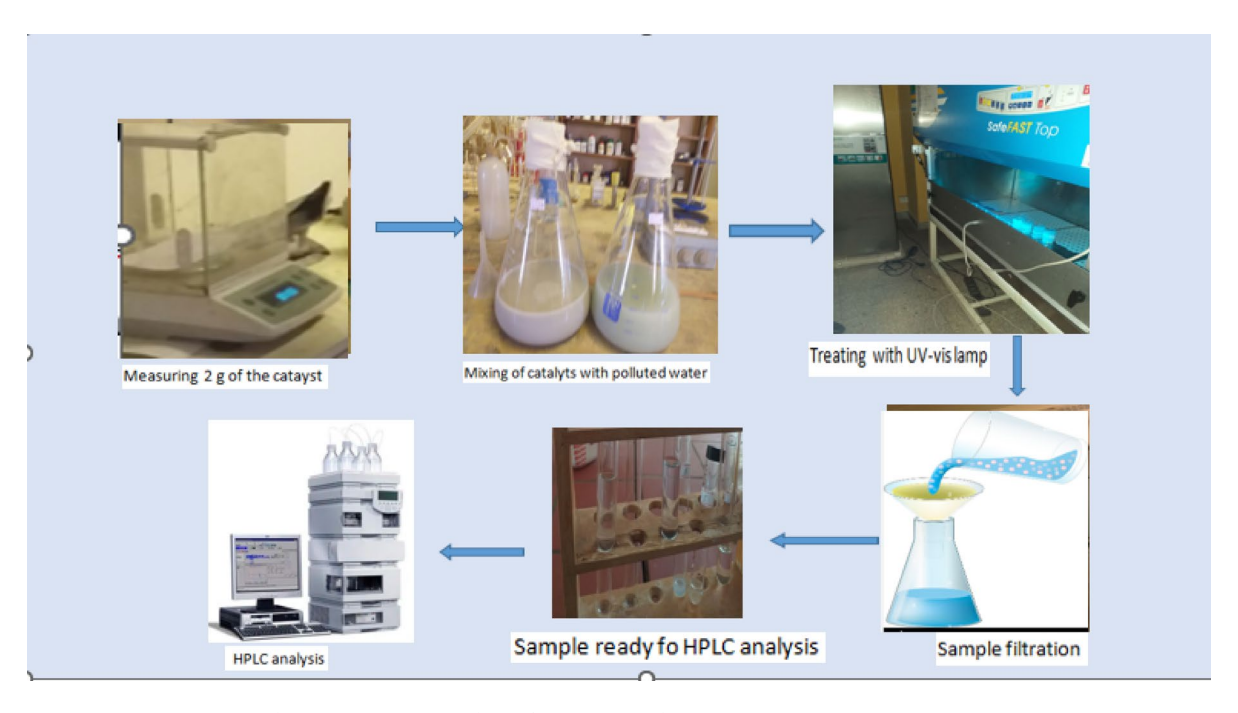


Fig. 1. Sample preparation Procedures for HPLC analysis.

together, reducing the active surface area and ultimately impairing photocatalytic activity 28 . The appropriate molar ratio selection of ${\rm TiO}_2$ –CuO–clay composite is also vital. Different ratios can affect the physical and chemical properties of the catalyst, including its stability, reactivity, and overall efficiency in degrading pollutants. Finding the right combination of these factors is essential for optimizing photocatalytic performance.

XRD analysis

The crystalline structure of the TiO_2 –CuO–clay soil composite was analyzed using X-ray diffraction (XRD) methods. The XRD results showed that the composite with a molar ratio of 4:3:5 exhibited distinct crystalline properties at 2 θ values of 15°, 25°, 38°, 42°, 49°, 50°, and 55° (Fig. 2). These angles correspond to peaks at (445), (450), (510), (750), (860), and (1290). In contrast, the composite with a molar ratio of 2:3:7 displayed its crystalline characteristics at 2 θ values of 13°, 26°, 48°, 54°, and 56°, with corresponding peaks at (600), (700), (1480), and (2520) (Fig. 2).

The XRD analysis provides valuable insights into the crystalline nature of the TiO₂–CuO–clay soil composite. The presence of sharp and distinct peaks indicates well-defined crystalline phases, which is important for photocatalytic activity. Crystallinity is often associated with enhanced electron mobility and improved photocatalytic performance. The differences in peak positions and intensities between the two molar ratios (4:3:5 and 2:3:7) suggest variations in the crystallization behavior and phase composition of the composites. The higher intensity peaks observed in the 4:3:5 ratio indicates a more stable crystalline structure, which may contribute to its superior photocatalytic properties, as reported in the literature²⁹.

The variations in peak positions can also provide insights into how the different molar ratios affect the photocatalytic capabilities of the composite. The 4:3:5 ratio, with its more pronounced peaks, may facilitate better light absorption and electron-hole pair generation, leading to more effective pollutant degradation.

The current study indicates the crystalline orientation of the materials through the increasing intensity observed in the peaks. The TiO₂ anatase phase usually occurs at 2θ = 25.3°, 37.8°, 48.0° and for CuO 2θ = 32.5°, 35.5°, 38.7° and 48.7°. The clay soil broad peaks were frequently found at 12°, 20°, and 26°. According to the literature report, the XRD results confirmed the presence of TiO₂–CuO–clay soil crystallites in the composite samples³⁰. The distinct peak pattern observed in the composite materials is primarily attributed to their crystalline nature. The sharpness of the XRD peaks highlights the purity and crystallinity of the TiO₂–CuO–clay soil nanocomposites, with high-intensity peaks being useful for determining crystal size. Using the Scherer equation (D=K\(\lambda\)/B cos\(\theta\)), the average crystalline size for the most intense diffraction peak of the TiO₂–CuO–Clay soil composite was found to be 8.29 nm. This size aligns with the crystalline size reported by^{28,79} which ranges from 8 to 37 nm for similar materials. The crystalline phase of the TiO₂–CuO–clay soil nanocomposite was identified as anatase by the XRD data. The composite materials' photocatalytic activity was examined in relation to the breakdown of phenol in aqueous solution exposed to UV light (280 nm). It has been discovered that the addition of the TiO₂–CuO–clay soil nanocomposite greatly increased photocatalytic efficiency.

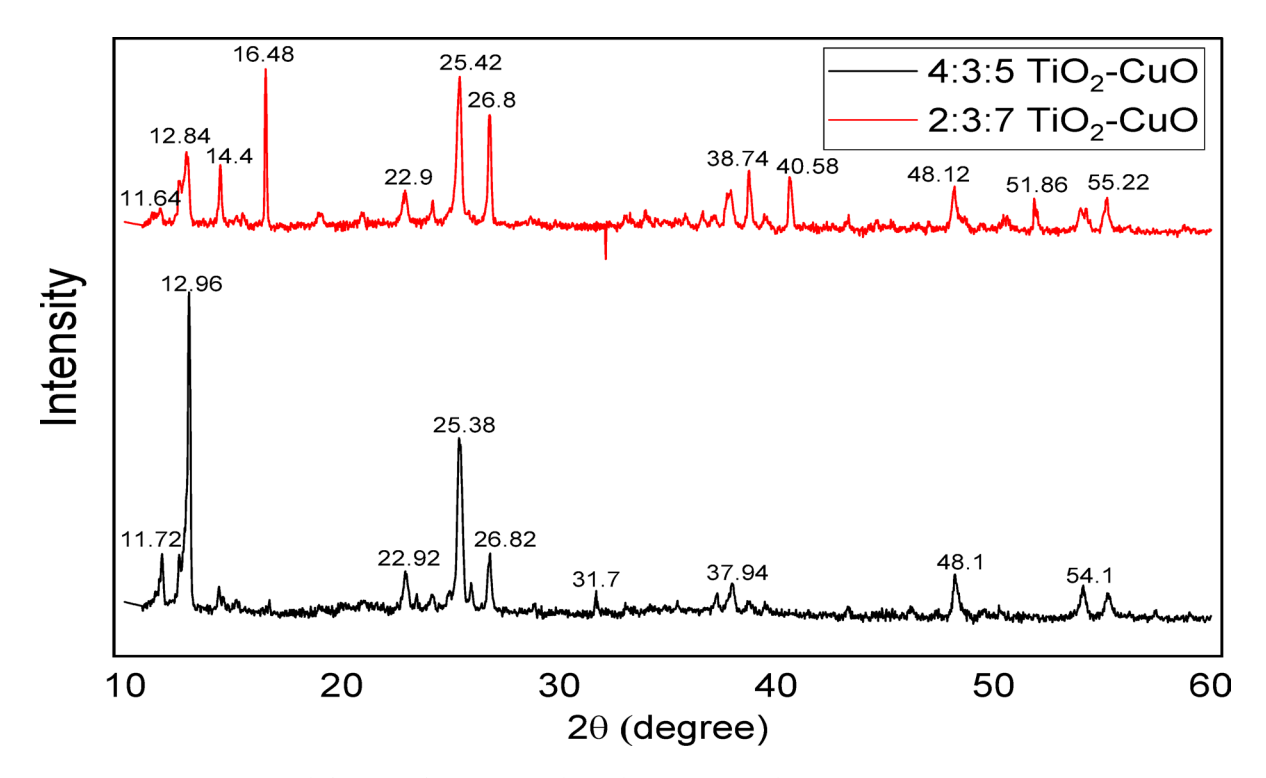


Fig. 2. X-ray diffraction of TiO₂-CuO-clay soil composite catalyst.

BET surface area analysis TiO₂-CuO-clay soil nanocomposite

The BET analysis clearly illustrates the variations in surface area characteristics of the TiO₂–CuO–clays soil nanocomposites, emphasizing how composition affects the performance of the materials. The TiO₂–CuO–clays soil nanocomposites varying surface characteristics were clearly shown by the BET characterization. The specific surface area of TiO₂–CuO–clay soil nanocomposites were analyzed at 28 °C using a Horiba surface area analyzer with model number of SA9603 (USA). The surface areas of the composites were determined to be 235 m²/g and 298 m²/g, respectively for 2:3:7 and 4:3:5 TiO₂–CuO–clay soil nanocomposites. The analysis shows that, the composite ratio of 4:3:5 TiO₂–CuO–clay nanocomposite was higher porous than 2:3:7 TiO₂–CuO–clay nanocomposite. The nanocomposite with higher surface area offers more active sites for photocatalytic reactions and improving pesticides degradations³¹. The increased surface area leads to increased number of actives sites that available for removal of pesticides from wastewater.

SEM analysis

The SEM images depict that, the TiO_2 –CuO–Clay soil nanocomposites were at two different molar ratios: A represents a ratio of 2:3:7, while B corresponds to a 4:3:5 ratio (Fig. 3). The analysis revealed that the grain sizes for the composites were 20 μ m for the 2:3:7 ratio and 10 μ m for the 4:3:5 ratio. This is why the grain size is in the micrometer range from 10 to 20 μ m; the composite is classified as a nanocomposite. Thus, the grain sizes of images A and B were different, 20 μ m and 10 μ m, respectively. This image not only illustrates the particle sizes but also provides insights into the surface structures of the electro-catalysts.

Figure 3a shows the selected area electron diffraction (SAED) patterns of the TiO₂-CuO-clay soil composites. The images indicate a higher degree of crystallization than Fig. 3b in the particles, suggesting that the synthesis process effectively maintained the crystalline structure of the materials. This information is crucial for understanding the performance characteristics of the electrocatalysts in various applications³².

FT-IR analysis

Fourier Transform Infrared (FT-IR) spectroscopy was employed to validate the effectiveness of the molecular imprinting process and to characterize the crystal phases of the synthesized oxides. In the present study, the FT-IR spectrum was recorded in the range of 4000–400 cm⁻¹ (Fig. 5). The spectra of both molar ratios, 2:3:7 (black line) and 4:3:5 (purple line), exhibit similar features and patterns. However, the spectrum for the 2:3:7 ratio shows a shorter intensity at 3272 cm⁻¹ compared to the more pronounced peak at 3438 cm⁻¹ for the 4:3:5 ratio. These peaks correspond to the stretching vibrations of O–H, which arise from metal hydroxyl groups or hydroxyl groups from crystallization water (Fig. 4). This finding shows that the broad bands at 3272 cm⁻¹ and 3438 cm⁻¹ indicates the presence of hydroxyl functionalities in both catalysts.

Additionally, the bending vibrations of O–M–O (specifically, the O–Ti–O or O–Cu–O) corresponded to the bands between 468 and 686 cm $^{-1}$, particularly showing distinct characteristics in the 4:3:5 molar ratio. In contrast, the M–O (Ti–O or Cu–O) vibrations for the 2:3:7 molar ratios are represented by bands between 400 and 600 cm $^{-1}$ as indicated by the green line. These observations align with findings from previous studies of the bending vibrations for the bands between 827 and 821 cm $^{-1}$ and 750 and 490 cm $^{-1}$ reported by 33,34 .

UV-vis analysis

The UV–vis absorption result indicated that, the ${\rm TiO_2-CuO}$ –clay soil composite has a peak observed at 375 nm (Fig. 5). The finding is consistent with 35 , who noted that the absorbance for crystalline particles is significantly lower than that of nanoparticles, which exhibit surface Plasmon resonance. There are significant absorption shifts from 450 to 375 nm. This shift is likely a result of the dense coating of ${\rm TiO_2}$ on the surfaces of CuO and clay soil particles, which enhances the material's absorption capacities within the UV–visible spectrum.

A B

| Igh-vac. SED PC-std. 15 kV x 1000 20/07/2023 High-vac. SED PC-std. 15 kV x 2000 20/07/2023 High-vac. SED PC-std. 15 kV x 2000 20/07/2023

Fig. 3. SEM image of the synthesized TiO₂-CuO-clay soil nanocomposite.

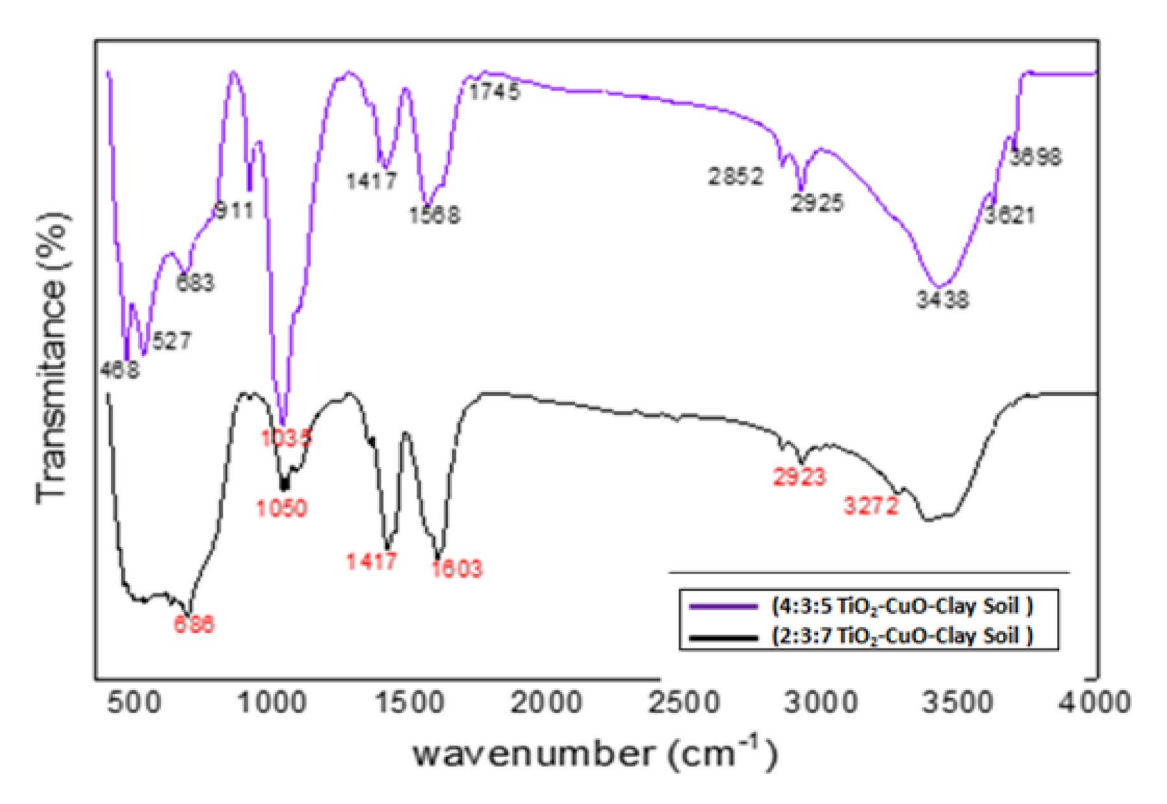
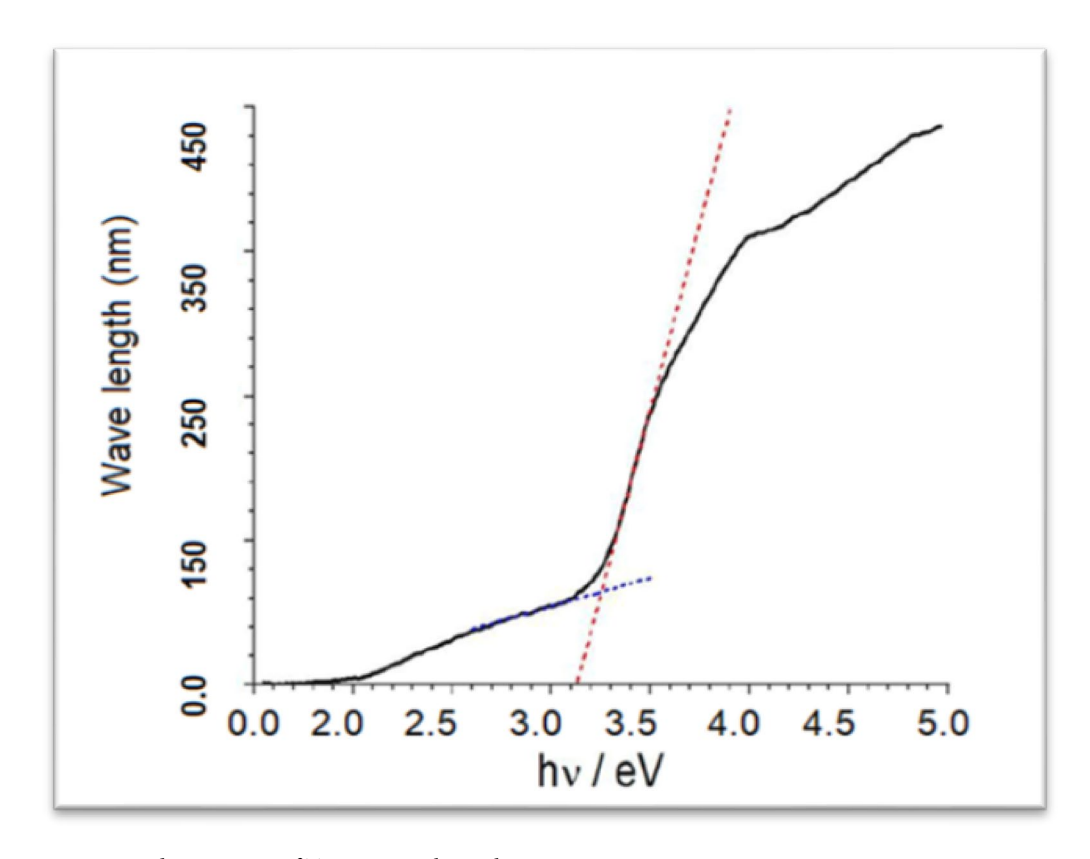


Fig. 4. FT-IR characterizations of TiO₂–CuO–clay soil composite.



 $\textbf{Fig. 5}. \ \ \text{Band gap energy of TiO}_2\text{--CuO--clay soil composites}.$

This modifications not only improves the optical properties of the composite but also its photocatalytic efficiency. The findings align with research highlighting the potential of ${\rm TiO}_2$ -based composites to facilitate faster phtodegradations of pollutants³⁶. Furthermore, the enhanced absorption characteristics are relevant for applications in water quality detection³⁷.

The UV-vis absorption spectra for the $\rm TiO_2$ -CuO-clay soil composite, in the 2:3:7 and 4:3:5 ratios, exhibit a range from 150 to 450 nm, with a peak light absorbance observed around 350 nm (Table 2). For the 2:3:7 ratio, the absorbance values were relatively low, starting at 0.09 at 150 nm and peaking at 0.095 at 350 nm, indicating limited light absorbance, while transmittance decreased correspondingly. In contrast, the 4:3:5 ratio exhibits significantly higher absorbance across all wavelengths, particularly peaking at 0.194 at 350 nm, suggesting a stronger capacity for light capture. This higher absorbance correlates with lower transmittance values within the visible spectrum, reflecting the $\rm TiO_2$ -CuO-clay soil nanocomposite's enhanced effectiveness in light absorption. This characteristic suggests its potential significance for photocatalytic applications, as noted in previous studies³⁸.

The findings highlighted the effectiveness of TiO₂-CuO-clay composites in light absorption, particularly within the UV-visible range. The significant absorption shift, coupled with enhanced performance due to the coating of TiO₂, suggests that such composite materials could be optimized for photocatalytic applications³⁸. Such optimization could lead to significant advancements in environmental remediation techniques, particularly in the degradation of pollutants under UV-vis light. In line with previous studies, the ability of TiO₂-based composites to harness light more effectively enhances their photocatalytic capability, facilitating the breakdown of harmful substances in various environmental settings^{38,39}. This characteristic aligns with in-water quality detection studies³⁷.

The findings revealed that the band gap energy of the TiO_2 –CuO–clay soil composite was determined to be approximately 3.54 eV (Fig. 5), as calculated using the Kubelka–Munk band gap energy formula. This value exceeds the typical band gap energy of TiO_2 reported in the literature which is 3.2 eV⁴⁰. This higher band gap energy enhances the solar photocatalytic activity of the TiO_2 –CuO–clay composites in the degradation of 2,4-D from contaminated water. This suggests that the composite can effectibley absorb light in the visible spectrum, making it suitable for photocatalytic applications.

A study indicates that the TiO₂ alone has inherent limitations in photocatalytic applications, such as low efficiency under visible light and rapid recombination of electron–hole pairs⁴¹. These factors hinder its effectiveness in environmental remediation, indicating a need for improvement. In the present study, the TiO₂–CuO–clay nanocomposite shows a significant band gap energy of 3.54 eV, which is higher than that of TiO₂. This enhanced band gap energy enables the composite to effectively utilize a broader spectrum of UV–vis radiation for photocatalytic processes⁴². A higher band gap often leads to increased energy absorption, which can enhance the generation of charge carriers (electrons and holes) necessary for photocatalytic reactions. This property is vital for degrading pollutants like 2,4-D, a common herbicide found in polluted water bodies. The findings also reveal that the combination of TiO₂, CuO and clay soil not only modifies the band gap energy structure but also enhances the photocatalytic efficiency. The successful degradation of 2,4-D illustrates the practical application of the composite in environmental remediation.

The absorbance value increases with wavelength up to about 450 nm, indicating effective light absorbance in the UV–visible region. The composite with 4:3:5 ratio of TiO₂:CuO:clay soil composites exhibits slightly higher absorbance than the 2:3:5 ratio, suggesting that the 4:3:5 ratio may have enhanced photocatalytic properties due to improved light absorption (Fig. 6). This variation emphasizes the influence of composition ratio on the optical characteristics and potential photocatalytic efficiency.

Effect of catalyst dose

To investigate the impact of catalyst dose on the photocatalytic degradation of pesticides, a series of experiments were conducted using prepared samples with an optimal pH solution, appropriate particle concentration, doped particles, and exposure to ultraviolet light at optimal light intensity³⁵. At $p^H \approx 4$, the concentrations of surface water and industrial wastewater were 35.10 µg/L and 157.63 µg/L, respectively. The efficiency of the photocatalytic degradation process showed significant improvement with increasing exposure times of 2, 5, 7, and 9 h. Notably, the removal efficiency continued to rise steadily up to 9 h. This enhancement can be attributed to the periodic reduction of pesticide concentrations and the increased generation of free radicals with longer

Ratio of TiO ₂ -CuO-clay soil	Absorbance	Transmittance	Wavelength (nm)
	0.09 ± 0.012	64±0.23	150
2:3:7	0.094 ± 0.30	63 ± 0.11	250
2.3.7	0.095 ± 0.20	62.5 ± 0. 30	350
	0.097 ± 0.31	62.10 ± 0.25	450
	0.190 ± 0.40	89±0.85	150
4:3:5	0.191 ± 0.31	90 ± 0.20	250
4.5.5	0.194 ± 0.51	90±0.56	350
	0.197 ± 0.31	82±0.35	450

Table 2. UV-vis absorbance and wavelength of TiO₂-CuO-clay soil composites.

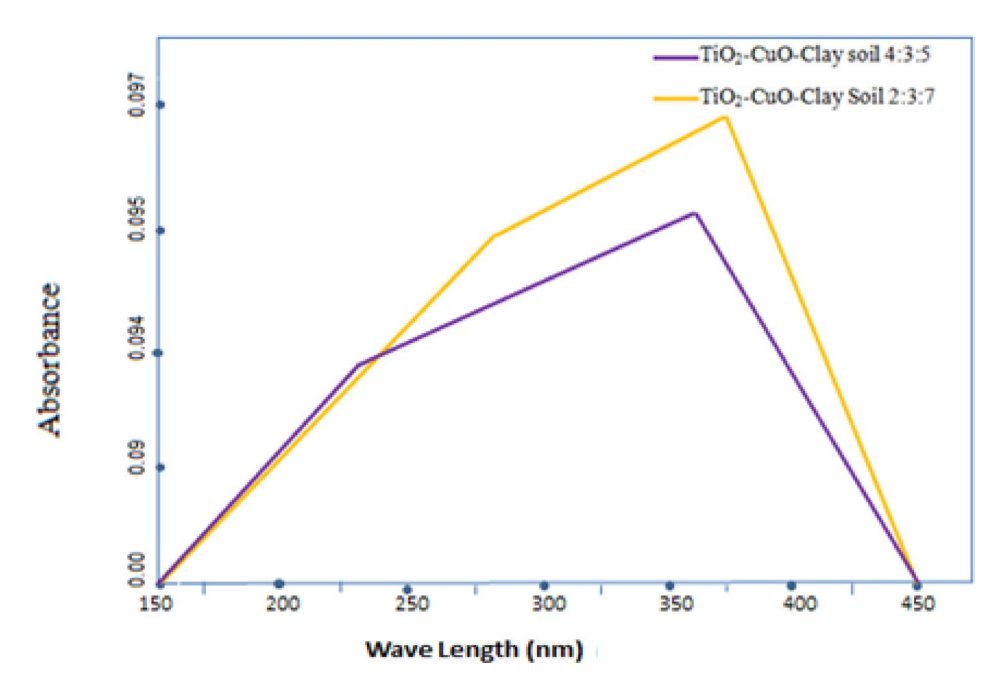


Fig. 6. UV-vis absorbance spectra of TiO₂-CuO-clay soil composites at two different ratios.

	TiO ₂ -CuO-clay so ratios (2:3:7)	il composites	TiO ₂ -CuO-clay so ratios (4:3:5)	il composites	res TiO ₂		CuO	
Irradiation time (hours)	Surface water (%)	Wastewater (%)	Surface water (%)	Wastewater (%)	Surface water (%)	Wastewater (%)	Surface water (%)	Wastewater (%)
2	94.4	96.94	95.18	97.90		X		х
5	94.58	97.16	95.27	99.10		41.5		39.72
7	94.87	98.49	95.49	99.58		63.8		49.31
9	95.38	98.72	96.20	99.84		85.01		67.23

Table 3. Degradations of 2,4-D from Surface and industrial wastewater using TiO₂-CuO-clay soil composites ratios (2:3:7, 4:3:5), CuO and TiO₂.

exposure times, which facilitates the oxidation of pesticide metabolites. Additionally, the stability and chemical composition of the pesticides may influence the time required for effective degradation⁴³.

The impact of the injected catalyst on the degradation of 2,4-D was evaluated by varying irradiation times under a UV–Vis spectroscopy lamp. In this study, the highest degradation rates were observed at 9 h of irradiation time. As shown in Table 3, the percentage of 2,4-D degradation, in a 2:3:7 ratio, increased with longer irradiation times, rising from 94.40 to 95.38% and from 96.94 to 98.72%, for surface water and industrial wastewater, respectively, with a constant catalyst dose. Similarly, for the 4:3:5 ratio in Table 3, degradation rates increased from 95.18 to 96.20% and from 97.9 to 99.84% for surface water and industrial wastewater, respectively, with increased irradiation time. Notably, these findings demonstrate that the composite catalyst is more effective than CuO and TiO₂ alone, which achieved degradation rates of approximately 67.23% and 85.01%, respectively.

The effect of the catalyst injected on variations of times, the degradation of 2,4-D under a UV–vis spectroscopy lamp, and the highest degradations was seen at 9 h of irradiation time. The percentage degradation of 2,4-D increases with increasing irradiation time from 94.40 to 95.38% and 96.94 to 98.72%, for surface water and industrial wastewater, respectively with a constant catalyst dose of 2 g. The same is true for B (4:3:5 ratio); the degradation of 2,4-D increases from 95.18 to 96.20% and 97.9 to 99.84%, respectively, with irradiation time. It is more effective than CuO and ${\rm TiO}_2$ photocatalytic degradations of 2,4 D from industrial wastewater, which is about 67.23% and 85.01%, respectively.

Effect of molar ratio

The result showed that the percentage degradations of 2,4-D by the TiO₂-CuO-clay soil composite were effectively degraded by the 4:3:5 catalyst molar ratios, which were 96.20% and 99.84% respectively, from surface water and industrial effluent, respectively (Table 3). The degradation efficiency of the TiO₂-CuO-clay soil composite increased with increasing catalyst molar ratios and increasing irradiation times⁴⁴.

The synthesis mixture TiO₂-CuO-clay soil molar ratio of 4:3:5 and constant calcination temperature of 720 °C were optimum conditions for 2,4-D photocatalytic degradation activities under UV-vis spectroscopy

light irradiations. For this case, the 4:3:5 molar ratio of the ${\rm TiO}_2$ –CuO–Clay soil composite at a calcination temperature of 720 °C was further used for the photocatalytic degradation of pesticides from the surface and industrial wastewater. According to the literature, the rate of pesticide degradation increased in proportion to the mass of the catalyst, and the optimal amount, as expressed in gram of catalyst per liter of solution was equivalent to 2.5 g/L⁴⁵.

Effect of surface water and industrial wastewater concentration

The concentration of 2,4-D, at a constant catalyst dose of 2 g/L polluted water, was found to be a significant factor influencing the degradation of pesticides from contaminated water, particularly in conjunction with irradiation time. After 9 h of irradiation time, the degradation of 2,4-D concentrations was markedly effective and dropped from 35.10 to 1.62 μ g/L for the TiO₂–CuO–clay soil composite at a (2:3:7) ratio, and to 1.34 μ g/L for the (4:3:5) ratio (Supplementary Fig. 1). Similarly, CuO and TiO₂ photocatalytic processes also resulted in significant reductions of 2,4-D concentrations. The surface water Concentrations of 2,4-D was decreased from 35.10 to 16.23 μ g/L with CuO and 35.10 to 12.45 μ g/L with TiO₂. In Industrial wastewater, the reduction was from 157.63 to 51.65 μ g/L for CuO and 157.63 to 23.63 μ g/L for TiO₂ (Supplementary Fig. 1A–C).

The results emphasize the critical role of initial 2,4-Ď concentration and catalyst dosage in determining the efficacy of photocatalytic degradation. The substantial reduction of 2,4-D levels after 9 h of irradiation time highlights the effectiveness of the TiO₂-CuO-clay composites, achieving nearly complete degradation at the optimal ratios. The comparison with CuO and TiO₂ alone reveals that the composite catalysts not only enhance the degradation efficiency but also provide a more effective solution for treating higher concentrations of pesticides, which is in agreement with the reports by Babu et al. ⁴³. The significant decrease in 2,4-D concentrations underscores the potential of these composite materials for practical applications in environmental remediation.

The same trend was observed with industrial wastewater from pesticide factories, where the concentrations of 2,4-D decreased dramatically from 157.63 μ g/L to 2.01 μ g/L and 0.24 μ g/L for catalytic molar ratios of 2:3:7 and 4:3:5, respectively (Supplementary Fig. 2). This significant reduction in initial 2,4-D concentrations correlates with a marked improvement in pesticide removal efficiency. In contrast, with the initial concentrations of 2,4-D, the concentration decreased from 35.10 to 1.34 μ g/L and from 157.68 to 0.24 μ g/L in surface water and industrial wastewater, respectively. According to data reported by Balakrishnan et al.²¹, the degradation efficiency of the catalyst increases from 65 to 86% with increasing concentrations of TiO₂ from 1 to 5 g/L. The specific molar ratio suggests tailored approach to optimize the reaction conditions for maximum degradation efficiency.

Kinetics of TiO₂-CuO-clay soil composite photocatalytic degradations of 2,4-D pesticide

In this study, the kinetics of photocatalytic degradation of 2,4-D using a TiO_2 –CuO–clay soil composite was investigated through varying time intervals, revealing significant insights into the degradation process. The photocatalytic degradation of 2,4-D was investigated with initial concentrations of 35.10 µg/L for surface water and 157.68 µg/L for industrial wastewater, using a catalyst loading of 2.0 g, at 2 h of irradiation, the final concentration of 2,4-D dropped to 4.82 µg/L, resulting in a Ln (Co/Cf) value of 3.4. As the irradiation time increased to 5 h, the final concentration further decreased to 4.47 µg/L, yielding a Ln (Co/Cf) value of 3.6. The trend continued with a final concentration of 2.37 µg/L, at 7 h and 2.01 µg/L, at 9 h, corresponding to Ln (Co/Cf) values of 4.2 and 4.4, respectively (Table 4). The weak linear fit, (R² of 0.693), rejects that the hypothesis that degradation process follows first-order kinetics (Fig. 7). The composite demonstrates enhanced photocatalytic activity in pollutant breakdown of pollutants, suggesting that the degradation of 2,4-D by TiO_2 –CuO–clay soil composite may occur through the hybrid reaction pathway. This process involves second order degradation, clay adsorption coupled with direct photocatalytic degradation.

These results shows that, the degradation rate of 2,4-D follows a pseudo-first-order kinetic model, where the rate of degradation is proportional to the concentration of the pesticide remaining in the solution. The increased Ln (Co/Cf) value with time suggests that the rate of degradation accelerates as the concentration of 2,4-D decreases, reflecting the efficiency of the composite in facilitating photocatalytic degradation process. The rapid decline in pesticide levels within the first few hours indicates a high initial reaction rate, which can be attributed to the generation of reactive species under UV irradiation that effectively decomposes the pesticide molecule. This finding was consistent with the pseudo-first-order kinetics for 2,4-D degradation ^{46,47}. The kinetic studies examining the absorption and degradation processes during the photocatalytic degradation of 2,4-D were performed using a batch reactor under UV irradiation.

Numerous researchers^{47,48}, have utilized the modified Langmuir–Hinshelwood (L–H) kinetic expression to study the kinetics of heterogeneous photocatalytic reactions effectively. To accurately characterize the solid–liquid interactions, the data obtained from solar photocatalysis experiments conducted under optimal conditions have been analyzed using a modified L–H kinetic model. This approach enhances the understanding of the reaction mechanisms. The findings of the current study are consistent with previous studies demonstrating the enhanced

Time (hr.)	C _o (μg/L)	C _f (µg/L)	$\operatorname{Ln}\left(\operatorname{C_o/C_f}\right)$
2	157.63	4.82	3.4
5	157.63	4.47	3.6
7	157.63	2.37	4.2
9	157.63	2.01	4.4

Table 4. First order kinetic model for degradation of 2,4-D by TiO₂-CuO-clay soil.

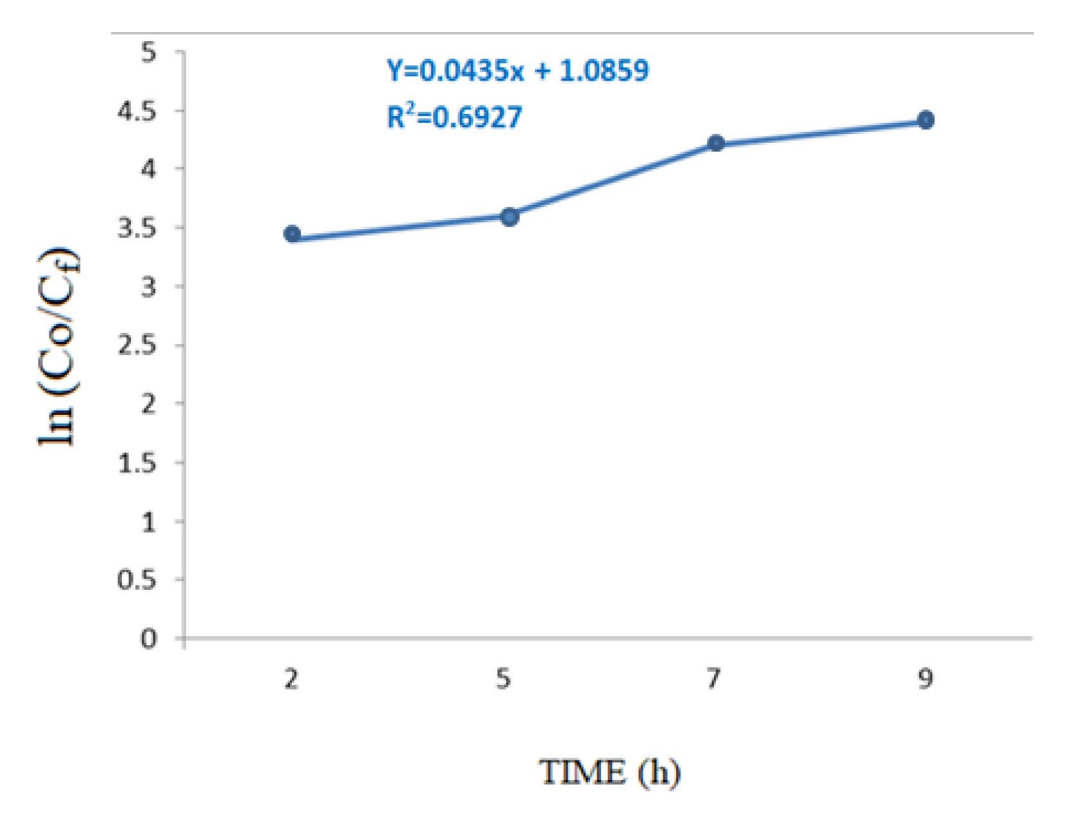


Fig. 7. Kinetics of 2,4-D degradation by TiO₂-CuO-clay soil composite.

photocatalytic activity of composite materials in environmental applications^{45,46}, emphasizing the importance of optimizing catalytic formulations for effective pollutant removal.

Comparison of photocatalytic activities ratio

The photocatalytic activity of the material was assessed by tracking the rate of 2,4-D degradation when exposed to UV–Vis light in the presence of the photocatalyst. The comparison of photocatalytic activities across various molar ratios of the same catalysts was evaluated based on their reaction rates and degradation efficiencies. This analysis provides insights into how different catalyst compositions influence the effectiveness of the photocatalytic process.

The photocatalytic degradation efficiency of the TiO_2 –CuO–clay soil composite under UV light was evaluated by comparing the degradation of 2,4-D at initial concentrations of 35.10 μ g/L from surface water and 157.68 μ g/L from industrial wastewater, using a catalyst loading of 2 g/L. This was also compared to the degradation efficiencies of CuO and TiO_2 alone. The TiO_2 –CuO–clay soil composite with a molar ratio of 4:3:5 demonstrated superior effectiveness in degrading 2,4-D compared to the composite with a 2:3:7 ratio (Fig. 6). This indicates that the specific composition of the catalyst significantly influences its photocatalytic performance⁴⁹.

The overall degradation of 2,4-D from surface water and industrial wastewater in the presence of the $\rm TiO_2$ –CuO–clay soil catalyst was observed over a period of 9 h and achieved an impressive efficiency of 99.84% when treating industrial wastewater. This result indicates that the $\rm TiO_2$ –CuO–clay soil composite photocatalyst, particularly at a molar ratio of 4:3:5, exhibits significantly higher degradation efficiency compared to the 2:3:7 ratio, as well as compared to CuO and $\rm TiO_2$ alone. According to 50, the degradation efficiencies for $\rm TiO_2$ and CuO were approximately 67.23% and 85.01%, respectively. These values highlight that the $\rm TiO_2$ –CuO–clay soil composite offers a markedly superior removal efficiency, demonstrating its potential as an effective photocatalyst for environmental remediation.

Degradation efficiency of TiO₂**–CuO–clay soil composite in surface water and industrial waste** To verify the effectiveness of the photocatalytic process in removing 2,4-D from surface water and industrial wastewater, experiments were conducted under controlled conditions using UV–Vis light, HPLC analysis, and TiO_2 –CuO–clay soil composites as catalysts. A 150 W xenon arc lamp emitting light at a wavelength of 280 nm served as the UV–Vis spectroscopy radiation source for the experiments. The HPLC setup included an injection volume of 1.0 mL, utilizing an Agilent capillary column with dimensions of 30 m × 250 mm × 0.25 mm, operating at a pressure of 9.3825 psi and a temperature of 80 °C. This systematic approach ensured accurate measurement of 2,4-D degradation and confirmed the efficacy of the photocatalytic process under the specified conditions.

The TiO_2 –CuO–clay soil composite effectively degraded 2,4-D concentrations to 1.34 μ g/L and 0.24 μ g/L from surface water and industrial waste, respectively, after 9 h of irradiation (Fig. 8). The enhanced photocatalytic degradation of 2,4-D in the UV/ TiO_2 –CuO–clay soil system can be attributed to the interactions between light-

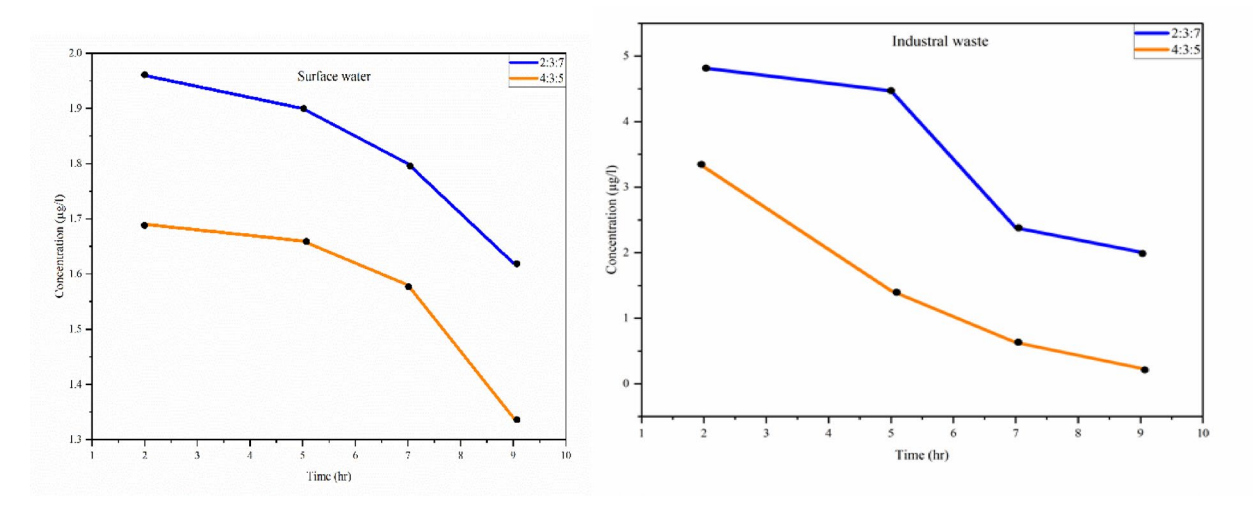


Fig. 8. Photo catalytic degradation efficiency of TiO₂-CuO-clay soil composite.

emitting photons and electrons in the semiconductor layer. According to the studies reported^{5,51}, the interaction between light-emitting photons and electrons interaction increases electron energy, facilitating energy transfer from the conduction band that exceeds the membrane capacity. As a result, positive holes and negatively charged electrons are generated, which can participate in chemical reactions. This mechanism shows the effectiveness of the composite in promoting photocatalytic activity and highlights the importance of optimizing catalyst properties for enhanced degradation efficiency.

The photocatalytic degradation of pesticides from surface water using TiO₂–CuO–clay soil composites has shown promising effectiveness. These catalysts were able to successfully remove 2,4-D from both surface water and industrial waste produced by the pesticide factory, as reported⁵². The study highlights how pesticide concentrations varied at different irradiation times and the final concentrations achieved after photocatalytic treatment, demonstrating the composite's significant ability to reduce pesticide levels. This underscores its potential as a viable solution for environmental remediation in contaminated water sources (Fig. 7).

Under UV–Vis light, the photocatalytic degradation efficiencies of 2,4-D pesticides from surface water and actual factory effluents were compared using TiO₂–CuO–clay soil composite photocatalysts⁵³. The initial concentrations of 2,4-D were 35.10 μg/L from surface water and 157.63 μg/L from pesticide factory effluent, with a catalyst loading of 2 g. Among the catalytic molar ratios tested, 2:3:7 and 4:3:5, the 4:3:5 TiO₂–CuO–clay soil composite demonstrated effectiveness in degrading 2,4-D. This finding indicates that optimizing the catalyst composition can significantly enhance its photocatalytic performance, making it a promising option for reducing pesticide contamination in various water sources.

The reported efficiencies of 96.18% and 99.84% highlight the potential of using the ${\rm TiO_2-CuO-clay}$ soil composite for treating different types of contaminated water. The high degradation rates in both surface water and industrial wastewater suggest that this composite is versatile and effective across varying conditions. The efficiency of 96.18% indicates that a significant portion of 2,4-D was effectively degraded, making this method a promising solution for agricultural runoff and other environmental concerns related to pesticide contamination. The nearly complete degradation (99.84%) of 2,4-D in industrial wastewater demonstrates the potential for this technology in treating effluents from pesticide manufacturing or usage, where concentrations of pollutants may be much higher.

The findings underscore the potential of using photocatalytic techniques for environmental remediation, particularly in the context of agricultural and industrial pollution 5456 . The combination of TiO_2 , CuO , and clay soil not only enhances the photocatalytic activity but also provides a sustainable approach to water treatment. Utilizing naturally occurring clay as a support material for TiO_2 and CuO can reduce costs and environmental impacts associated with more traditional water treatment methods.

Photocatalytic mechanisms

The photocatalysis mechanism of 2,4-D (2,4-Dichlorophenoxyacetic acid) degradation during the reaction follows these steps: Absorption of light energy, where titanium dioxide (TiO₂), copper oxide (CuO), and clay soil absorb light energy (hv) from a light source. This energy excites an electron (e⁻) from the valence band (VB) of both TiO₂ and CuO into the conduction band (CB), leaving behind positively charged holes (h⁺) in the VB.

$$TiO_2 + CuO + hv \rightarrow TiO_2 (e^-CB + h^+VB) + CuO (e^-CB + h^+VB)$$

Formation of reactive species

The photogenerated holes (h^+) in the valence band of TiO₂ and CuO can react with water (H_2O) or hydroxide ions (OH⁻) adsorbed on the composite surface, producing hydroxyl radicals (OH). Meanwhile, the photo generated

Fig. 9. Schematic photocatalytic degradation mechanism of 2,4-D.

electrons (e⁻) in the conduction band can react with oxygen molecules (O_2) adsorbed on the nanocomposite surface, generating superoxide radicals (O_2 ⁻⁻) (Fig. 9).

$$\begin{split} &\mathrm{TiO_2-CuO-Clay}\,\left(h^+\mathrm{VB}\right) + \mathrm{H_2O} \rightarrow \mathrm{TiO_2-CuO-Clay} + \mathrm{OH^{\cdot}} + \mathrm{H^{+}} \\ &\mathrm{CuO-Clay}\,\left(h^+\mathrm{VB}\right) + \; \mathrm{H_2O} \rightarrow \mathrm{CuO-Clay} + \mathrm{OH^{\cdot}} + \mathrm{H^{+}} \\ &\mathrm{TiO_2-CuO-Clay}\,\left(e^-\mathrm{CB}\right) + \mathrm{O_2} \rightarrow \mathrm{TiO_2-CuO-Clay} + \mathrm{O_2^{\cdot-}} \end{split}$$

Pesticide degradation: Degradation of 2,4-D: The hydroxyl radicals (OH') and superoxide radical anions (O_2 -), which are powerful oxidizing agents, can react with 2,4-dichlorophenoxyacetic acid (2,4-D), breaking its molecular bonds and converting it into simpler, less toxic products such as CO_2 , H_2O , and other mineral acids. The degradation reaction mechanism occurs on the clay soil surface (Fig. 8).

Conclusion

The degradation of pesticides in surface water and industrial wastewater has been extensively studied in laboratory settings using various photocatalytic methods. This study focused on a $\rm TiO_2-CuO$ -clays soil nanocomposite under UV irradiation to investigate the photocatalytic degradation of 2,4-D. The results indicated that the $\rm TiO_2-CuO$ -clay soil nanocomposite is a promising option for effectively degrading 2,4-D when exposed to UV light. The study found that a catalytic molar ratio of 4:3:5 $\rm TiO_2-CuO$ -clay soil nanocomposite was performed efficiently in an aqueous environment. Thus, the $\rm TiO_2-CuO$ -clays soil nanocomposite was successfully degraded 2,4-D from both surface water and industrial wastewater. Furthermore, the investigation revealed that factors such as catalyst major ratio, pollutant concentration, and irradiation time significantly influenced the photocatalytic degradation of 2,4-D from surface water and pesticide factory effluents.

Data availability

Data is provided with the manuscript, and in the Supplementary files.

Received: 20 May 2025; Accepted: 14 July 2025

Published online: 25 August 2025

References

- 1. Das, T. K. et al. Herbicides use in crop production: An analysis of cost-benefit, non-target toxicities and environmental risks. *Crop Prot.* 181, 106691. https://doi.org/10.1016/j.cropro.2024.106691 (2024).
- Catalá, R. & Salinas, J. Tailoring crop nutrition to fight weeds. Proc. Natl. Acad. Sci. 115(29), 7456–7458. https://doi.org/10.1073/pnas.1809311115 (2018).
- 3. Lopes, F. C. S. M. R., da Rocha, M. G. C., Bargiela, P., Sousa Ferreira, H. & Pires, C. A. D. M. Ag/TiO₂ photocatalyst immobilized onto modified natural fibers for photodegradation of anthracene. *Chem. Eng. Sci.* 227, 115939. https://doi.org/10.1016/j.ces.2020. 115939 (2020).
- 4. Li, Q., Wu, X., Zhang, Y. & Wang, Y. The effect of agricultural environmental total factor productivity on urban–rural income gap: Integrated view from China. *Sustainability* 12(8), 3327. https://doi.org/10.3390/su12083327 (2020).
- Fiorenza, R. et al. Preferential removal of pesticides from water by molecular imprinting on TiO₂ photocatalysts. Chem. Eng. J. 379, 122309. https://doi.org/10.1016/j.cej.2019.122309 (2020).
- Premnath, N. et al. A crucial review on polycyclic aromatic hydrocarbons—Environmental occurrence and strategies for microbial degradation. Chemosphere 280, 130608. https://doi.org/10.1016/j.chemosphere.2021.130608 (2021).
- 7. Teklu, B. M., Hailu, Å., Wiegant, D. A., Scholten, B. S. & Van den Brink, P. J. Impacts of nutrients and pesticides from small- and large-scale agriculture on the water quality of Lake Ziway, Ethiopia. *Environ. Sci. Pollut. Res.* 25(14), 13207–13216. https://doi.org/10.1007/s11356-016-6714-1 (2018).
- 8. Song, X.-P. et al. Massive soybean expansion in South America since 2000 and implications for conservation. *Nat. Sustain.* 4(9), 784–792. https://doi.org/10.1038/s41893-021-00729-z (2021).
- 9. Curchod, L. et al. Temporal variation of pesticide mixtures in rivers of three agricultural watersheds during a major drought in the Western Cape, South Africa. *Water Res. X* 6, 100039. https://doi.org/10.1016/j.wroa.2019.100039 (2020).

- 10. Margesin, R. & Schinner, F. Biodegradation and bioremediation of hydrocarbons in extreme environments. *Appl. Microbiol. Biotechnol.* **56**(5–6), 650–663. https://doi.org/10.1007/s002530100701 (2001).
- 11. Teshome, A. Pesticide Lifecycle in Ethiopia: Challenges, Opportunities and Leverage Points, no. 1.
- 12. Desta, H. Local perceptions of ecosystem services and human-induced degradation of lake Ziway in the Rift Valley region of Ethiopia. *Ecol. Indic.* 127, 107786. https://doi.org/10.1016/j.ecolind.2021.107786 (2021).
- 13. Merga, L. B., Mengistie, A. A., Alemi, M. T. & Van den Brink, P. J. Biological and chemical monitoring of the ecological risks of pesticides in Lake Ziway, Ethiopia. *Chemosphere* 266, 129214. https://doi.org/10.1016/j.chemosphere.2020.129214 (2021).
- Jansen, H. C. & Harmsen, J. Pesticide Monitoring in the Central Rift Valley 2009–2010: Ecosystems for Water in Ethiopia 44 (Alterra, 2011).
- Adejoro, S. A. Effects of the 2,4-dichlorophenoxyacetic acid (2,4-D) herbicide contamination on soil microbiology at the community level. J. Glob. Ecol. Environ. https://doi.org/10.56557/jogee/2022/v14i37439 (2022).
- 16. Islam, F. et al. Potential impact of the herbicide 2,4-dichlorophenoxyacetic acid on human and ecosystems. *Environ. Int.* 111, 332–351. https://doi.org/10.1016/j.envint.2017.10.020 (2018).
- 17. Shamsedini, N., Dehghani, M., Nasseri, S. & Baghapour, M. A. Photocatalytic degradation of atrazine herbicide with Illuminated Fe⁺³–TiO, nanoparticles. *J. Environ. Heal. Sci. Eng.* **15**(1), 7. https://doi.org/10.1186/s40201-017-0270-6 (2017).
- 18. El-Saeid, M. H., BaQais, A. & Alshabanat, M. Study of the photocatalytic degradation of highly abundant pesticides in agricultural soils. *Molecules* 27(3), 634. https://doi.org/10.3390/molecules27030634 (2022).
- Altendji, K. & Hamoudi, S. Efficient photocatalytic degradation of aqueous atrazine over graphene-promoted g-C₃N₄ nanosheets. Catalysts 13(9), 1265. https://doi.org/10.3390/catal13091265 (2023).
- Carbajo, J., García-Muñoz, P., Tolosana-Moranchel, A., Faraldos, M. & Bahamonde, A. Effect of water composition on the photocatalytic removal of pesticides with different TiO₂ catalysts. *Environ. Sci. Pollut. Res.* 21, 12233–12240. https://doi.org/10.10 07/s11356-014-3111-5 (2014).
- Tarekegn, M. M., Balakrishnan, R. M., Hiruy, A. M., Dekebo, A. H. & Maanyam, H. S. Nano-clay and iron impregnated clay nanocomposite for Cu²⁺ and Pb²⁺ ions removal from aqueous solutions. *Air Soil Water Res.* 15, 2023. https://doi.org/10.1177/117 86221221094037 (2022).
- 22. Yin, K., Liu, J., Vasilescu, A.-R., Di Filippo, E. & Othmani, K. A procedure to prepare sand-clay mixture samples for soil–structure interface direct shear tests. *Appl. Sci.* 11(12), 5337. https://doi.org/10.3390/app11125337 (2021).
- 23. Kubiak, A. et al. Microwave-assisted synthesis of a TiO₂-CuO heterojunction with enhanced photocatalytic activity against tetracycline. *Appl. Surf. Sci.* **520**, 146344. https://doi.org/10.1016/j.apsusc.2020.146344 (2020).
- 24. Andrade, P. H. M. et al. Band gap analysis in MOF materials: Distinguishing direct and indirect transitions using UV-vis spectroscopy. Appl. Mater. Today 37, 102094. https://doi.org/10.1016/j.apmt.2024.102094 (2024).
- 25. Saikumari, N., Dev, S. M. & Dev, S. A. Effect of calcination temperature on the properties and applications of bio extract mediated titania nano particles. Sci. Rep. 11(1), 1734. https://doi.org/10.1038/s41598-021-80997-z (2021).
- 26. Armaković, S. J. et al. Efficiency of La-doped TiO₂ calcined at different temperatures in photocatalytic degradation of β-blockers. *Arab. J. Chem.* 12(8), 5355–5369, https://doi.org/10.1016/j.arabic.2017.01.001 (2019).
- Arab. J. Chem. 12(8), 5355-5369. https://doi.org/10.1016/j.arabjc.2017.01.001 (2019).
 Mzimela, N., Tichapondwa, S. & Chirwa, E. Visible-light-activated photocatalytic degradation of rhodamine B using WO₃ nanoparticles. RSC Adv. 12(53), 34652-34659. https://doi.org/10.1039/D2RA06124D (2022).
- 28. Liu, Y. et al. Pt particle size affects both the charge separation and water reduction efficiencies of CdS-Pt nanorod photocatalysts for light driven H, generation. J. Am. Chem. Soc. 144(6), 2705-2715. https://doi.org/10.1021/jacs.1c11745 (2022).
- 29. Huang, S. et al. Tailoring of crystalline structure of carbon nitride for superior photocatalytic hydrogen evolution. *J. Colloid Interface Sci.* 556, 324, 334, https://doi.org/10.1016/j.icis.2019.08.060 (2019)
- Interface Sci. 556, 324–334. https://doi.org/10.1016/j.jcis.2019.08.069 (2019).
 Tekin, D., Birhan, D. & Kiziltas, H. Thermal, photocatalytic, and antibacterial properties of calcinated nano-TiO₂/polymer composites. Mater. Chem. Phys. 251, 123067. https://doi.org/10.1016/j.matchemphys.2020.123067 (2020).
- 31. Zeshan, M. et al. Remediation of pesticides using TiO₂ based photocatalytic strategies: A review. *Chemosphere* **300**, 134525. https://doi.org/10.1016/j.chemosphere.2022.134525 (2022).
- 32. Dong, C.-D., Chen, C.-W., Kao, C.-M. & Hung, C.-M. Synthesis, characterization, and application of CuO-modified TiO₂ electrode exemplified for ammonia electro-oxidation. *Process Saf. Environ. Prot.* 112, 243–253. https://doi.org/10.1016/j.psep.2017.05.016
- 33. Alkhabbas, M., Odeh, F., Alzughoul, K., Afaneh, R. & Alahmad, W. Jordanian Kaolinite with TiO₂ for improving solar light harvesting used in dye removal. *Molecules* 28(3), 989. https://doi.org/10.3390/molecules28030989 (2023).
- 34. Morjène, L. et al. New composite material based on Kaolinite, cement, TiO₂ for efficient removal of phenol by photocatalysis. *Environ. Sci. Pollut. Res.* 28(27), 35991–36003. https://doi.org/10.1007/s11356-021-13150-y (2021).
- 35. Zandsalimi, Y. et al. Photocatalytic removal of 2,4-dichlorophenoxyacetic acid from aqueous solution using tungsten oxide doped zinc oxide nanoparticles immobilized on glass beads. *Environ. Technol* 43, 1–36. https://doi.org/10.1080/09593330.2020.1797901 (2020).
- 36. Musial, J., Mlynarczyk, D. T. & Stanisz, B. J. Photocatalytic degradation of sulfamethoxazole using TiO₂-based materials—Perspectives for the development of a sustainable water treatment technology. *Sci. Total Environ.* **856**, 159122. https://doi.org/10.1016/j.scitotenv.2022.159122 (2023).
- Guo, Y., Liu, C., Ye, R. & Duan, Q. Advances on water quality detection by UV–Vis spectroscopy. Appl. Sci. 10(19), 6874. https://doi.org/10.3390/app10196874 (2020).
- 38. Napruszewska, B. D., Duraczyńska, D., Kryściak-Czerwenka, J., Nowak, P. & Serwicka, E. M. Clay minerals/TiO₂ composites—Characterization and application in photocatalytic degradation of water pollutants. *Molecules* 29(20), 4852. https://doi.org/10.3390/molecules29204852 (2024).
- 39. Zhang, Y. et al. TiO₂/BiOI p-n junction-decorated carbon fibers as weavable photocatalyst with UV-vis photoresponsive for efficiently degrading various pollutants. *Chem. Eng. J.* 415, 129019. https://doi.org/10.1016/j.cej.2021.129019 (2021).
- 40. Del Angel, R., Durán-Álvarez, J. C. & Zanella, R. TiO₂-low band gap semiconductor heterostructures for water treatment using sunlight-driven photocatalysis. In *Titanium Dioxide—Material for a Sustainable Environment* (InTech, 2018). https://doi.org/10.5772/intechopen.76501.
- 41. Abdelfattah, I. & El-Shamy, A. M. A comparative study for optimizing photocatalytic activity of TiO₂-based composites with ZrO₂, ZnO, Ta₂O₅, SnO, Fe₂O₃, and CuO additives. *Sci. Rep.* **14**(1), 27175. https://doi.org/10.1038/s41598-024-77752-5 (2024).
- 42. Pastrana-Martínez, L. M. et al. Photocatalytic activity of functionalized nanodiamond-TiO₂ composites towards water pollutants degradation under UV/Vis irradiation. *Appl. Surf. Sci.* **458**, 839–848. https://doi.org/10.1016/j.apsusc.2018.07.102 (2018).
- 43. Babu, S. G. et al. Synergistic effect of sono-photocatalytic process for the degradation of organic pollutants using CuO–TiO₂/rGO. *Ultrason. Sonochem.* **50**, 218–223. https://doi.org/10.1016/j.ultsonch.2018.09.021 (2019).
- 44. Çinar, B. et al. Hydrothermal/electrospinning synthesis of CuO plate-like particles/TiO₂ fibers heterostructures for high-efficiency photocatalytic degradation of organic dyes and phenolic pollutants. *Mater. Sci. Semicond. Process.* 109, 104919. https://doi.org/10.1016/j.mssp.2020.104919 (2020).
- 45. Herrmann, J. M. & Guillard, C. Photocatalytic degradation of pesticides in agricultural used waters. *I. R. l'Acad. Sci. Ser. IIc Chem.* 3(6), 417–422. https://doi.org/10.1016/S1387-1609(00)01137-3 (2000).
- Hadei, M. et al. A comprehensive systematic review of photocatalytic degradation of pesticides using nano TiO₂. Environ. Sci. Pollut. Res. 28(11), 13055–13071. https://doi.org/10.1007/s11356-021-12576-8 (2021).

- Akbari Shorgoli, A. & Shokri, M. Photocatalytic degradation of imidacloprid pesticide in aqueous solution by TiO₂ nanoparticles immobilized on the glass plate. Chem. Eng. Commun. 204(9), 1061–1069. https://doi.org/10.1080/00986445.2017.1337005 (2017).
- 48. Kundu, S., Pal, A. & Dikshit, A. K. UV induced degradation of herbicide 2,4-D: Kinetics, mechanism and effect of various conditions on the degradation. Sep. Purif. Technol. 44(2), 121–129. https://doi.org/10.1016/j.seppur.2004.12.008 (2005).
- 49. Wang, Y. et al. Hollow nanoboxes Cu_{2-x}S@ZnIn₂S₄ core-shell S-scheme heterojunction with broad-spectrum response and enhanced photothermal-photocatalytic performance. Small 18(31), 2202544. https://doi.org/10.1002/smll.202202544 (2022).
- Navakoteswara Rao, V. et al. Photocatalytic recovery of H₂ from H₂S containing wastewater: Surface and interface control of photo-excitons in Cu₂S@TiO₂ core-shell nanostructures. Appl. Catal. B Environ. 254, 174–185. https://doi.org/10.1016/j.apcatb.20 19.04.090 (2019).
- 51. Zafar, H. et al. CuO and ZnO nanoparticle application in synthetic soil modulates morphology, nutritional contents, and metal analysis of *Brassica nigra*. ACS Omega 5(23), 13566–13577. https://doi.org/10.1021/acsomega.0c00030 (2020).
- 52. Fiorenza, R. et al. Preferential removal of pesticides from water by molecular imprinting on TiO₂ photocatalysts. *Chem. Eng. J.* 379, 122309. https://doi.org/10.1016/j.cej.2019.122309 (2020).
- 53. Ismael, A. M. et al. Novel TiO₂/GO/CuFe₂O₄ nanocomposite: a magnetic, reusable and visible-light-driven photocatalyst for efficient photocatalytic removal of chlorinated pesticides from wastewater. RSC Adv. 10(57), 34806–34814. https://doi.org/10.1039/D0RA02874F (2020).
- 54. Danish, M. S. S. et al. Photocatalytic applications of metal oxides for sustainable environmental remediation. *Metals (Basel)* 11(1), 80. https://doi.org/10.3390/met11010080 (2021).
- Alfano, O. M., Brandi, R. J. & Cassano, A. E. Degradation kinetics of 2,4-D in water employing hydrogen peroxide and UV radiation. Chem. Eng. J. 82(1-3), 209-218. https://doi.org/10.1016/S1385-8947(00)00358-2 (2001).
- Hu, G. et al. Recent developments and challenges in zeolite-based composite photocatalysts for environmental applications. Chem. Eng. J. 417, 129209. https://doi.org/10.1016/j.cej.2021.129209 (2021).

Acknowledgements

The author would like to acknowledge Addis Ababa University, research director for financing the research grant. The authors also would like to acknowledge Mr. Michael Girimay for technical support.

Author contributions

The author declare that all authors have participated in (a) conception and design, or analysis and interpretation of the data; (b) drafting the article or revising it critically for important intellectual content; and (c) approval of the final version.

Funding

Addis Ababa University, Research Directorate, Grant Number GSR/0622/2021.

Declarations

Competing interests

The authors declare no competing interests.

Additional information

Supplementary Information The online version contains supplementary material available at https://doi.org/1 0.1038/s41598-025-11814-0.

Correspondence and requests for materials should be addressed to T.A.T.

Reprints and permissions information is available at www.nature.com/reprints.

Publisher's note Springer Nature remains neutral with regard to jurisdictional claims in published maps and institutional affiliations.

Open Access This article is licensed under a Creative Commons Attribution-NonCommercial-NoDerivatives 4.0 International License, which permits any non-commercial use, sharing, distribution and reproduction in any medium or format, as long as you give appropriate credit to the original author(s) and the source, provide a link to the Creative Commons licence, and indicate if you modified the licensed material. You do not have permission under this licence to share adapted material derived from this article or parts of it. The images or other third party material in this article are included in the article's Creative Commons licence, unless indicated otherwise in a credit line to the material. If material is not included in the article's Creative Commons licence and your intended use is not permitted by statutory regulation or exceeds the permitted use, you will need to obtain permission directly from the copyright holder. To view a copy of this licence, visit https://creativecommons.org/licenses/by-nc-nd/4.0/.

© The Author(s) 2025